

Eddy covariance measurements of the sea spray aerosol flux over the open ocean

Sarah J. Norris,¹ Ian M. Brooks,¹ Martin K. Hill,¹ Barbara J. Brooks,¹ Michael H. Smith,¹ and David A. J. Sproson¹

Received 12 July 2011; revised 24 February 2012; accepted 4 March 2012; published 12 April 2012.

[1] Direct eddy covariance measurements of size-segregated sea spray aerosol fluxes over the open Atlantic Ocean are presented, along with a source function derived from them for a wind speed range of 4 to 18 m s⁻¹ and a size range of 0.176 < R_{80} < 6.61 μm . This is in broad agreement with other recent estimates of the source function over this size range but shows a more rapid decrease with size above $R_{80} = 2 \mu\text{m}$ than most other functions. The measurements were made during a 3 week cruise in the North Atlantic as part of the UK contribution to the international Surface Ocean–Lower Atmosphere Study (SOLAS) program. They utilized the new high-rate Compact Lightweight Aerosol Spectrometer Probe (CLASP), providing a 16-channel size spectrum (0.17 < R_{amb} < 9.5 μm) at 10 Hz, collocated with a sonic anemometer. The measurements demonstrate the high variability in sea spray aerosol flux compared with other air-sea fluxes, both between individual estimates and in the scales contributing to the flux.

Citation: Norris, S. J., I. M. Brooks, M. K. Hill, B. J. Brooks, M. H. Smith, and D. A. J. Sproson (2012), Eddy covariance measurements of the sea spray aerosol flux over the open ocean, *J. Geophys. Res.*, 117, D07210, doi:10.1029/2011JD016549.

1. Introduction

[2] Sea-salt aerosols, produced from breaking waves and their resulting whitecaps, are the largest single source of aerosol mass injected into the atmosphere from the surface after windblown dust [Hoppel *et al.*, 2002]. Interest in large particles (radius at 80% relative humidity, $R_{80} > 1 \mu\text{m}$) originated in their potential to influence the air-sea fluxes of heat and water vapor, and their impact on visible and infrared propagation [Doss-Hammel *et al.*, 2002]. More recently interest has grown in the role of smaller sea spray aerosol within the climate system via their impact on radiative transfer. They are the dominant source of scattering for solar radiation under clear-sky conditions over the open oceans [Haywood *et al.*, 1999] and are an important source of cloud condensation nuclei influencing the microphysical properties of marine stratocumulus, a significant source of uncertainty in climate predictions. Sea salt also plays a role in chemical processes in the marine boundary layer [O'Dowd *et al.*, 1999; Sørensen *et al.*, 2005] and can provide a substantial sink for atmospheric trace gases [O'Dowd *et al.*, 2000]. In order to include the effects of sea spray within numerical models, an accurate parameterization of the surface aerosol flux is required – the sea spray source function.

[3] A wide range of source functions have been proposed, spanning about 6 orders of magnitude [Andreas, 1998, 2002], although this large variability has been reduced to

within about 1 order of magnitude among the most recent studies for particles with R_{80} between about 0.1 and 10 μm [O'Dowd and de Leeuw, 2007; de Leeuw *et al.*, 2007, 2011]. Almost all sea spray source functions have been derived via indirect techniques; the most widely used of which is the measurement of the mean size spectra and an assumption of equilibrium so that production can be inferred from the dry deposition rate, which is assumed to be well defined by previous studies [e.g., Fairall *et al.*, 1983; Fairall and Larsen, 1984; Smith *et al.*, 1993; Hoppel *et al.*, 2002]. This approach has been shown to be inappropriate for small particles because the rate of dry deposition is very low and thus the lifetime of particles in the air is much longer than the timescales associated with changes in concentration due to surface production or advection. A number of studies have derived a source function by using the fractional coverage of whitecaps as a function of wind speed to scale the measured aerosol spectrum produced over individual whitecaps; the latter have been estimated both from laboratory studies [Monahan *et al.*, 1982, 1986; Mårtensson *et al.*, 2003] and measurements within the surf zone [Clarke *et al.*, 2006]. It is worth noting, however, that the parameterizations proposed for whitecap fraction as a function of wind speed also suffer significant uncertainty, spanning 2 orders of magnitude [Anguelova and Webster, 2006]. Reid *et al.* [2001] estimated a source function from aircraft measurements of the changing aerosol concentration with fetch in a developing internal boundary layer. Recently, Petelski and Piskozub [2006] estimated a source function from measurements of the vertical gradient of aerosol concentration between 8 and 20 m and the flux-gradient relationships of Monin-Obukhov surface similarity theory. While this

¹School of Earth and Environment, University of Leeds, Leeds, UK.

approach has a more robust physical basis than the equilibrium technique, *Andreas* [2007] has questioned their omission of the von Kármán constant (≈ 0.4) from the flux-gradient relation which results in an increase in the flux estimate by a factor of 2.5. Also, Monin-Obukhov surface layer similarity has not yet been validated for aerosols.

[4] The most direct method for measuring turbulent fluxes is eddy covariance. This is a challenging measurement for sea spray aerosol: the typically low number concentration results in poor counting statistics, a worsening problem with increasing particle size and with finer size resolution of the measurement. The bulky nature of many aerosol instruments along with the need to site them within weatherproof enclosures often imposes a need for long sample lines which introduce a lag between the turbulent wind and aerosol measurements. This results in a loss of some of the highest-frequency fluctuations, and potentially a loss of larger particles to the walls of the sample line, compounding the issue of poor counting statistics and requiring estimation of a correction function. Many aerosol instruments, designed for mean concentration measurements, also sample too slowly (≤ 1 Hz) to resolve all the turbulent variability, resulting in underestimation of the eddy covariance flux.

[5] Only a handful of recent studies have attempted direct eddy covariance measurements of the sea spray particle flux. *Nilsson et al.* [2001] made eddy covariance estimates of the total flux of marine aerosols (dry radius, $R_{\text{dry}} > 5$ nm) over the Arctic Ocean using a sonic anemometer and a condensation particle counter (CPC). *Geever et al.* [2005] also utilized a CPC ($5 \text{ nm} < R < 0.5 \text{ }\mu\text{m}$) along with a Particle Measurement Systems (PMS) ASASP-X optical particle counter ($50 \text{ nm} < R < 0.5 \text{ }\mu\text{m}$) to make the first eddy covariance estimates of pseudo-size-segregated fluxes ($R > 5$ nm, and $R > 50$ nm) at Mace Head on the Atlantic coast of Ireland. The relative humidity for which these particle size ranges apply was not stated. Both *Nilsson et al.* [2001] and *Geever et al.* [2005] derive a source flux by adding an estimated deposition flux to the measured net flux. *de Leeuw et al.* [2007] utilized a PMS PCASP to measure the particle concentration after heating the inflow to 300°C in an attempt to volatilize all except the sea-salt component of the aerosol. Net eddy covariance fluxes were then estimated for particles in 4 coarse and overlapping size ranges ($R_{80} = 0.055\text{--}0.075$, $0.075\text{--}0.095$, $0.055\text{--}0.1875$, and $0.055\text{--}0.45 \text{ }\mu\text{m}$). *Norris et al.* [2008] made net eddy flux measurements of particles segregated into 6 size bins with mean radii (R_{80}) 0.15, 0.16, 0.19, 0.24, 0.5, and $1.2 \text{ }\mu\text{m}$ using an early version of the Compact Lightweight Aerosol Spectrometer Probe (CLASP). This data set was too limited to derive a robust source function directly from the eddy covariance fluxes, but the results were consistent with recent estimates of the sea spray source function.

[6] With the exception of *Nilsson et al.* [2001], the previous eddy covariance estimates of sea spray aerosol fluxes have all been made at coastal sites. Here we present the first direct eddy covariance measurements of size-segregated aerosol fluxes over the open ocean.

2. Measurements

[7] Eddy covariance measurements of aerosol fluxes were obtained during cruise D317 of the RRS *Discovery*,

21 March to 12 April 2007. They were made as part of the Sea Spray, Gas Flux and Whitecaps (SEASAW) project, one of several UK contributions to the international Surface Ocean–Lower Atmosphere Study (SOLAS) concerned with physical exchanges at the air-sea interface [*Brooks et al.*, 2009]. The cruise took place in the northeast Atlantic (Figure 1), departing from Govan on the west coast of Scotland and ending in Lisbon, Portugal.

[8] A primary focus was to obtain measurements in high-wind conditions; to this end the ship relocated every few days to sample within low-pressure systems crossing the Atlantic. At each location measurements were made with the ship hove to with the bow into wind. Flux estimates were obtained for mean wind speeds between approximately 4 and 18 m s^{-1} and significant wave heights up to approximately 5 m . Biological activity was not measured but satellite derived estimates indicate net primary production was low ($< 0.4 \text{ gC m}^{-2} \text{ day}^{-1}$) throughout the flux measurements. Aerosol volatility measurements indicated that the organic content of the aerosol was also low.

2.1. Mean Conditions

[9] Mean meteorological measurements were obtained from the ship's permanently installed instrumentation: a Vaisala WA15 anemometer, Vaisala HMP45 temperature and humidity probe, and Vaisala PTB100A barometer. Water temperature and salinity were measured with a Falmouth Scientific OTM and OCM sensors – both part of the ship's permanent core instrumentation – with water pumped from an inlet approximately 5 m below the surface. Wave state was measured with a shipborne wave recorder [*Tucker and Pitt*, 2001].

2.2. Aerosol Measurement

[10] Instrumentation for the measurement of turbulent fluxes was installed at the top of the foremast of the RRS *Discovery*, 21.3 m above the surface; it consisted of a Gill R3 sonic anemometer, a Licor LI-7500 open path gas analyzer, and a new version (mk.3) of the CLASP instrument [*Hill et al.*, 2008]. This is an improved version of the instrument used by *Norris et al.* [2008]; it measures a 16-channel size spectrum at ambient humidity covering the size range $0.17 < R_{\text{amb}} < 9.5 \text{ }\mu\text{m}$ at a sample rate of 10 Hz . Measuring just $25 \times 8 \times 5 \text{ cm}$, the unit is small enough to site at the base of the sonic anemometer, allowing a very short sample line, minimizing the lag time between the CLASP and the anemometer samples (here 0.2 s). The installation site necessitated sample inlet lines that were gently curved, with the inlet situated at the same level as, and approximately 0.4 m aft of the sonic anemometer head and facing forward into the prevailing wind [*Hill et al.*, 2008, Figure 9] and inclined downward at approximately 45° . The flow rate is actively controlled by onboard electronics, and recorded to allow subsequent correction of the particle spectra for any minor variations about the nominal flow rate of $50 \text{ cm}^3 \text{ s}^{-1}$. This flow rate is high compared to many other aerosol size spectrometers helping to achieve adequate counting statistics.

[11] The loss of particles to the walls of the inlet tube used was estimated following *Pui et al.* [1987] and a correction applied to the measured particle spectra. The correction modeled this specific configuration: the curve and radius

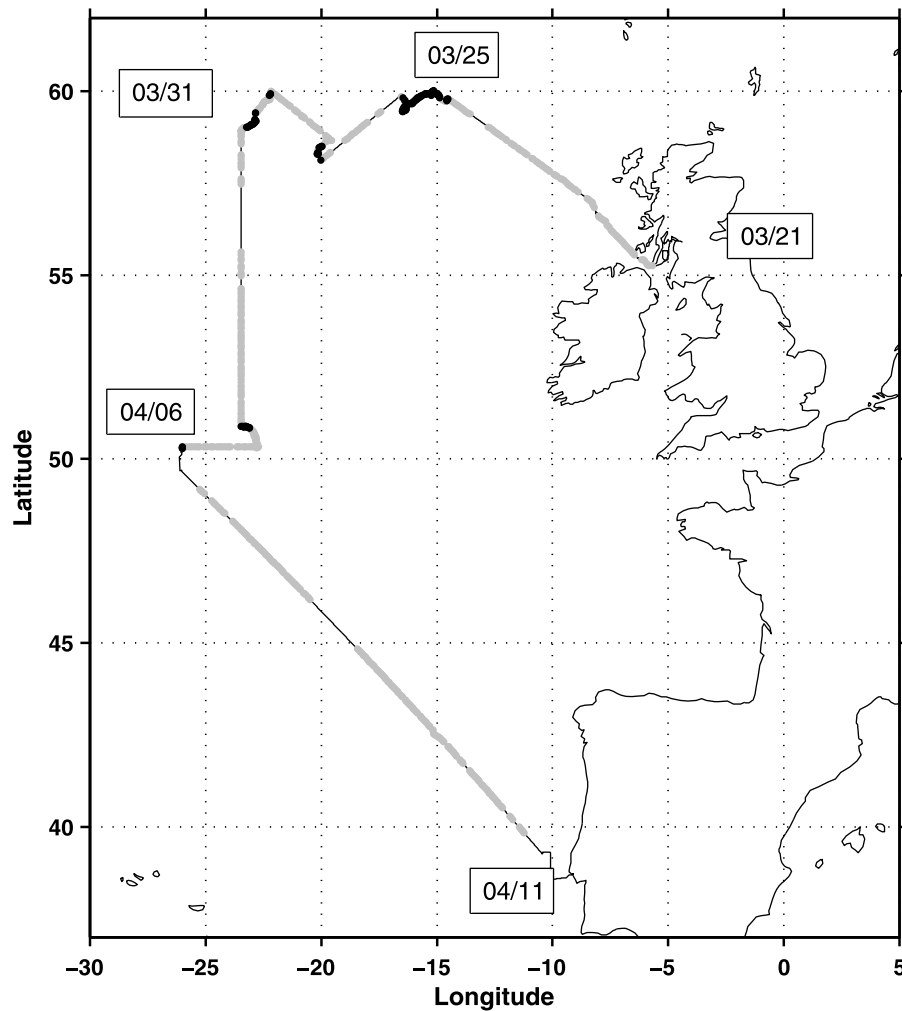


Figure 1. Map of the cruise track for cruise D317, sailing from Govan, Scotland, and finishing in Lisbon, Portugal. Dots mark the locations of individual flux estimates; black indicates that all quality control tests were passed, while gray indicates at least one test was failed; the majority of the latter are underway samples. The dates show the start and finish dates of the cruise along with the start date of measurements at each location along the cruise track.

of the two bends, air temperature of 10°C , measured flow rate of 55 mL s^{-1} , inlet length of 40 cm and an internal diameter of 4 mm. Figure 2 shows the calculated sampling efficiency with particle size: with losses ranging from 92% for the largest particles, with mean $R_{\text{amb}} = 8.5\ \mu\text{m}$, decreasing rapidly to 43% at $R_{\text{amb}} = 5.66\ \mu\text{m}$, 19% at $R_{\text{amb}} = 3.03\ \mu\text{m}$, and 0.1% at $R_{\text{amb}} = 0.22\ \mu\text{m}$. As a check on overall CLASP data quality the mean spectra, corrected for wall losses, were compared with those from a PMS PCASP situated in a container lab on the fo’c’sle deck. This drew its sample through an isokinetic inlet from a 49 mm diameter sample line with an inlet on the mast above the bridge at approximately the same level as the CLASP unit on the foremast; agreement within a factor 2 was found throughout most of the cruise (not shown). Note that unlike the PCASP, the flow path into the CLASP scatter cell is not constricted and thus the sample does not suffer the same acceleration and dynamic heating and associated drying; the relative humidity of the CLASP sample is thus very close to ambient

while that of the PCASP is lowered significantly to an estimated value of 20%. All size spectra are adjusted to a reference relative humidity of 80% via the *Lewis and Schwartz* [2006] growth model for sea salt for this intercomparison. Some uncertainty in this adjustment is inevitable since hygroscopic growth depends on the chemical composition of the aerosol. In particular there is evidence that organic enrichment of sea-salt aerosol affects the growth factors [*Saxena et al.*, 1995; *Saxena and Hildemann*, 1996; *Swietlicki et al.*, 1999]. Information about the aerosol composition inferred from volatility measurements indicates that the level of organics in the aerosol sampled was low; the sea-salt growth factors are thus assumed to be adequate. Some additional uncertainty will arise from using the growth model with particles that have effloresced. However, at 80% relative humidity the error in particle size resulting from the difference in the growth and the evaporation curves will be very small since sea-salt particles become homogenous solution droplets at 74% [*Tang et al.*, 1997]. Use of the eddy

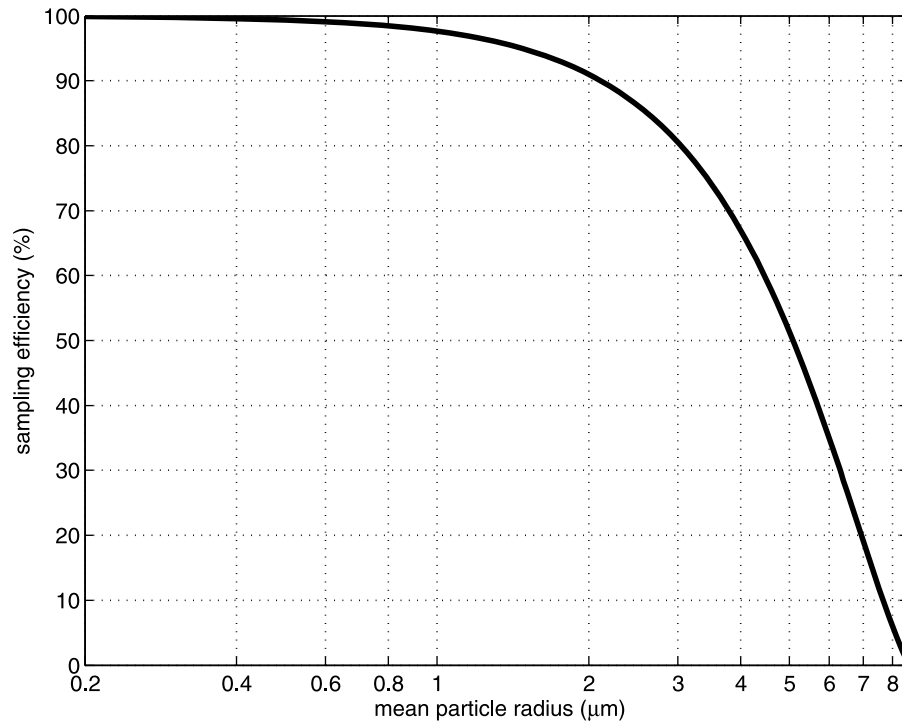


Figure 2. Compact Lightweight Aerosol Spectrometer Probe (CLASP) inlet sampling efficiency for the Sea Spray, Gas Flux and Whitecaps (SEASAW) cruise installation.

covariance technique requires correction of the measured turbulent wind components for both the changing attitude and motion of the ship [e.g., *Edson et al.*, 1998]. Ship motion was derived from a combination of three-axis linear accelerometers and angular rate gyros sampled at 20 Hz, coupled with the low-frequency heading and the mean platform velocity from the ship's navigation system [*Brooks*, 2008]. All instruments were interfaced via RS485 serial connections to a central logging system mounted in a weather proof enclosure on the foremast platform. The logging system was connected to the ship's network, and its clock was synchronized to a network time server, in turn synchronized to GPS time, on a regular schedule. In order to eliminate the possibility of an increasing phase shift between the instruments due to any small differences in their internal clock rates, logging intervals were limited to 70 min, after which all instruments were stopped and restarted together to resynchronize the timing.

2.3. Eddy Covariance Fluxes

[12] Eddy covariance fluxes were estimated over 28 min averaging intervals; this period was chosen on the basis of inspection of the cospectra for the momentum flux to ensure inclusion of all turbulence scales contributing to the flux. A total of 403 28 min turbulent wind records were obtained during the cruise, 319 of which have high-rate aerosol measurements available. Not all of these are suitable for flux estimates and a variety of quality control criteria are applied to exclude poor quality records retaining 111 for the final flux analysis.

[13] Initially only records where the wind direction is within 30° of the bow and the ship is hove to (mean ship

velocity $< 1 \text{ m s}^{-1}$) are accepted; this restricts the data set to conditions for which the mean flow distortion over the *RRS Discovery* has been modeled and corrections to the mean wind speed and effective height are available [*Yelland et al.*, 1998, 2002]. Individual ogive functions [*Friehe et al.*, 1991; *Brooks and Rogers*, 2000] for the momentum flux were inspected to ensure that only records where the cospectra were well behaved were accepted [*Fairall et al.*, 1997].

[14] Figure 3 shows ogive curves for the flux of particles with mean $R_{\text{amb}} = 0.35$ (channel range 0.29 to 0.41) μm from 9 consecutive 28 min records, along with their mean, under conditions with a steady wind of approximately 11 m s^{-1} ; the ogives for the corresponding momentum fluxes are shown for comparison. The momentum flux estimates show variability about the mean that is typical of such measurements, and reflects the stochastic nature of turbulent fluxes. 95% of the flux results from frequencies $> 0.01 \text{ Hz}$, which corresponds to scales shorter than about 1100 m. The aerosol flux displays both greater variability between individual estimates than the momentum flux, and greater variability in the flux contributions from different frequencies within a given record. This higher variability is attributed to the discrete surface source of the aerosol – individual whitecaps. The spatial separation of breaking wave crests depends upon the sea state and wind speed, but may be of the order of 100 m or more. This imposes a strong, irregular heterogeneity on the surface source, on scales similar to those of the dominant flux-carrying eddies, that does not exist for the flux of momentum or scalars such as heat and water vapor. The mean of the aerosol flux ogives over the 5 h period smooths out most of this variability and closely approximates the shape of the momentum flux ogive curves; this

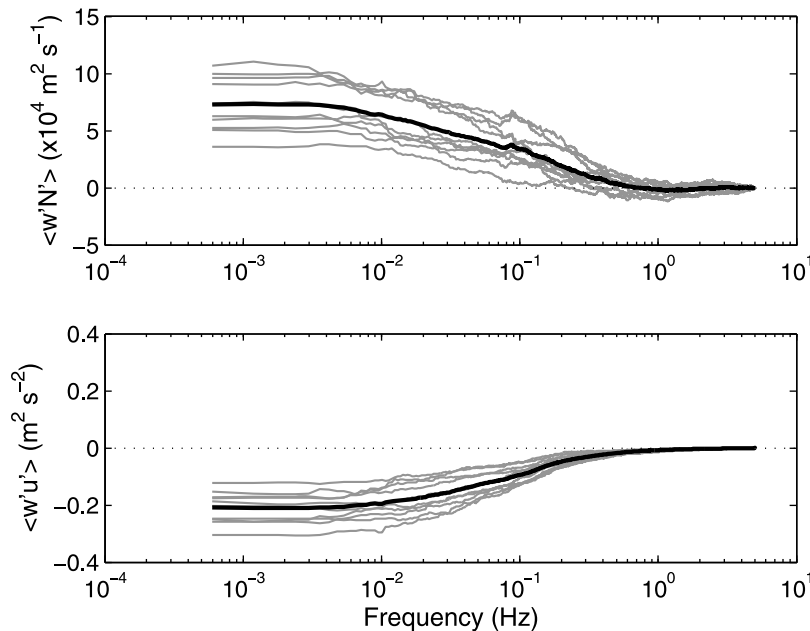


Figure 3. Ogive curves for nine consecutive 28 min records of (top) aerosol flux for particles with mean radius at $R_{\text{amb}} = 0.35 \mu\text{m}$ (channel range of 0.29–0.41 μm) and (bottom) the corresponding momentum fluxes at a mean wind speed of 11 m s^{-1} on 24 March. The gray lines are the individual records; the black lines are the mean of all nine ogives in each case.

demonstrates that the mean aerosol flux contributions at different scales are similar to those for momentum.

[15] Reliable and representative estimates of the surface flux by eddy covariance requires homogeneous, stationary conditions and that any temporal trends in mean aerosol concentration or forcing conditions occur over timescales much longer than the flux averaging period. Over the open ocean forcing conditions are usually homogeneous on scales smaller than those associated with individual weather systems (~ 100 s of km) except in the vicinity of fronts (atmospheric or oceanic). As a result, the mean aerosol concentration is expected to be reasonably homogeneous except where advection from remote sources other than the sea surface results in significant horizontal gradients in concentration. Aerosol from non-sea spray sources will also have a different chemical composition and hygroscopic properties; this is important for adjustment of size spectra to a common reference humidity. For this reason otherwise acceptable flux estimates were discarded from the analysis where the total aerosol loading and air mass back trajectory indicated a polluted, continental air mass. A total of 201 flux estimates were rejected after all quality control assessments leaving 118 estimates, from the original 319, for the next stage of analysis.

[16] Limits to instrument temporal responses may result in an underestimation of the true flux; this is a significant problem if the response falls below 2–3 Hz [Buzorius *et al.*, 2000]. The magnitude of flux loss is estimated following Horst [1997] and a correction applied. For CLASP’s 10 Hz sample frequency in the conditions observed here this varies from a minimum of 1% at winds of 2 m s^{-1} to a maximum of 17% at 18 m s^{-1} .

[17] If the turbulent perturbations of particle numbers are small compared to the total concentration then the small

mean differences in air density resulting from temperature and humidity differences between upward and downward moving parcels of air may result in a biased flux estimate and a Webb correction should be applied to the fluxes [Webb *et al.*, 1980]. Here the Webb correction is small, $<1\%$ in over 70% of flux estimates, and has thus been neglected. This is consistent with Held *et al.* [2011] who also found the Webb correction to be small for eddy covariance estimates of total aerosol number fluxes over open leads in Arctic sea ice.

[18] Eddy covariance flux measurements of aerosol are complicated by the hygroscopic properties of the aerosol, which results in a change in size of the aerosol with relative humidity. Where the aerosol are sized at ambient humidity, as here, turbulent fluctuations in humidity may result in a bias in the measured particle flux in the direction of the humidity flux [Fairall, 1984; Fairall and Larsen, 1984; Kowalski, 2001]. We utilize high-rate humidity measurements from the LI-7500 to determine the turbulent fluctuations in relative humidity and correct the measured aerosol spectra at 10 Hz to the mean ambient relative humidity for each 28 min record using the Lewis and Schwartz [2006] parameterization of sea salt’s size dependence on relative humidity

$$CC \cong \left(\left(\frac{1 - RH_1}{2.0 - RH_1} \right)^{1/3} \right) / \left(\left(\frac{1 - RH_2}{2.0 - RH_2} \right)^{1/3} \right), \quad (1)$$

where CC is the ratio between particle size at RH_1 (measured RH) and RH_2 . Individual flux estimates are then calculated at the mean ambient humidity. Figure 4 shows the impact of the correction for the humidity flux induced bias on a single 28 min data record; the flux spectrum is shown both with

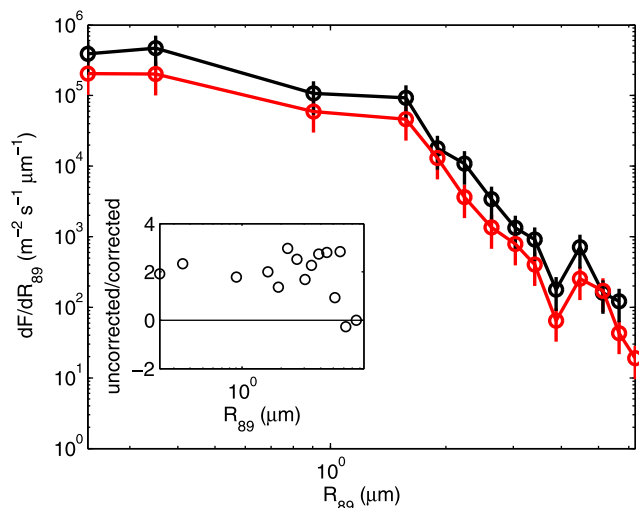


Figure 4. A single estimate of the particle flux spectrum corrected for the humidity flux induced bias (red line) and the uncorrected flux spectra (black line). The relative humidity for this record varied from 83% to 95%, with a mean of 89%; the water vapor flux was 0.012 g kg^{-1} . The error bars show the median standard error for the entire data set (30%). The inset shows raw uncorrected flux spectrum divided by the correct flux spectrum.

and without the correction along with the ratio of the raw to corrected flux spectra. In order to illustrate the significance of the bias the median standard error for the entire data set is indicated. For the majority of cases a positive (upward) bias was observed, consistent with a positive humidity flux. The corrected flux estimates varied from 82% down to 5% of the uncorrected values, with a mean of 46%, and a standard deviation of 30%. It was not possible to correct every flux estimate; the open path LI-7500 suffers from a number of problems that can degrade data quality, including precession of the optical chopper induced by gyroscopic effects as the ship pitches and rolls, distortion of the sampling head under imposed accelerations, and contamination of the optics by sea spray [Yelland *et al.*, 2009]. Seven aerosol flux estimates coincided with LICOR records that suffered from significant problems and could not be corrected for humidity bias. Of the initial 319 aerosol flux spectra estimates we are thus left with 111 corrected estimates were obtained from which to determine a source function.

[19] The individual aerosol flux spectra, although corrected for the humidity flux induced bias, are all valid at the mean ambient relative humidity for their respective averaging periods. In order to average multiple flux estimates and assess the dependency on wind speed, each flux spectrum must be adjusted to a fixed reference humidity – a value of 80% is widely used [de Leeuw *et al.*, 2011]. This adjustment is again made following Lewis and Schwartz [2006].

[20] An examination of the cospectra and ogive functions for representative periods across the full CLASP size range indicates that the absolute number concentrations are so low for particles in the four largest size channels (radii greater than $5.47 \mu\text{m}$ at ambient humidity) that their turbulent cospectra are dominated by Poisson noise and it is not

possible to make reliable eddy covariance flux estimates; these channels are thus omitted from the eddy covariance analysis reducing the range of sizes for which direct flux measurements are available.

3. Results

3.1. Mean Conditions

[21] The mean meteorological conditions for the period during which measurements were made are shown in Figure 5 along with the friction velocity, u_* , significant wave height, H_s , and total aerosol number concentration within the CLASP measurement range. The periods for which the aerosol flux estimates passed all quality control criteria are highlighted on the plots of u_* and total aerosol number concentration.

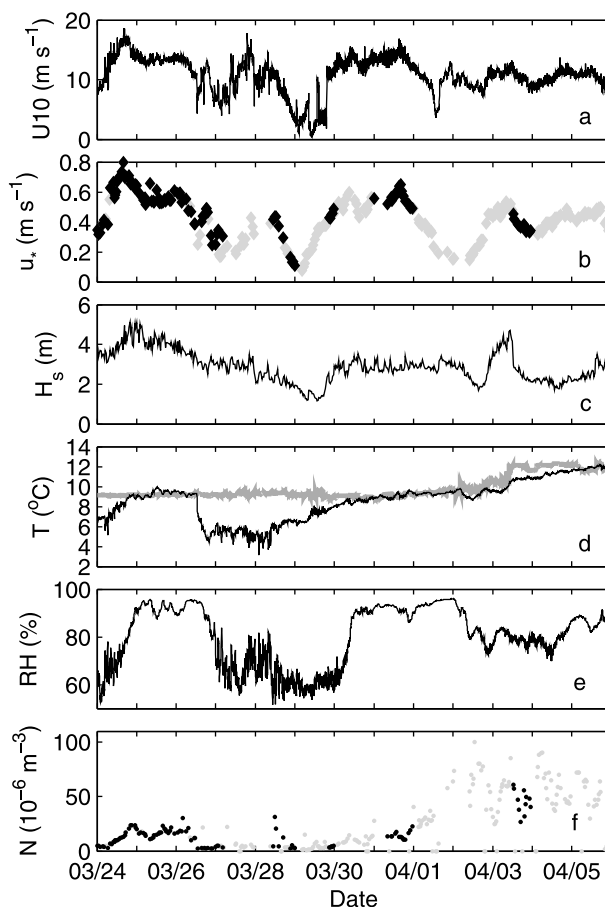


Figure 5. Time series of mean conditions during the cruise: (a) 10 m wind speed, U_{10} (m s^{-1}), (b) friction velocity u_* (m s^{-1}), (c) significant wave height, H_s (m), (d) temperature of the air at ~ 17 m (black line) and near-surface water (gray line) ($^{\circ}\text{C}$), (e) relative humidity (%), and (f) CLASP 28 min averages of total particle number concentration (m^{-3}). In Figures 5b and 5f, each symbol denotes a 28 min period where eddy covariance fluxes were estimated; black symbols indicate that all quality control criteria were passed, and gray symbols denote periods where the acceptance criteria were failed.

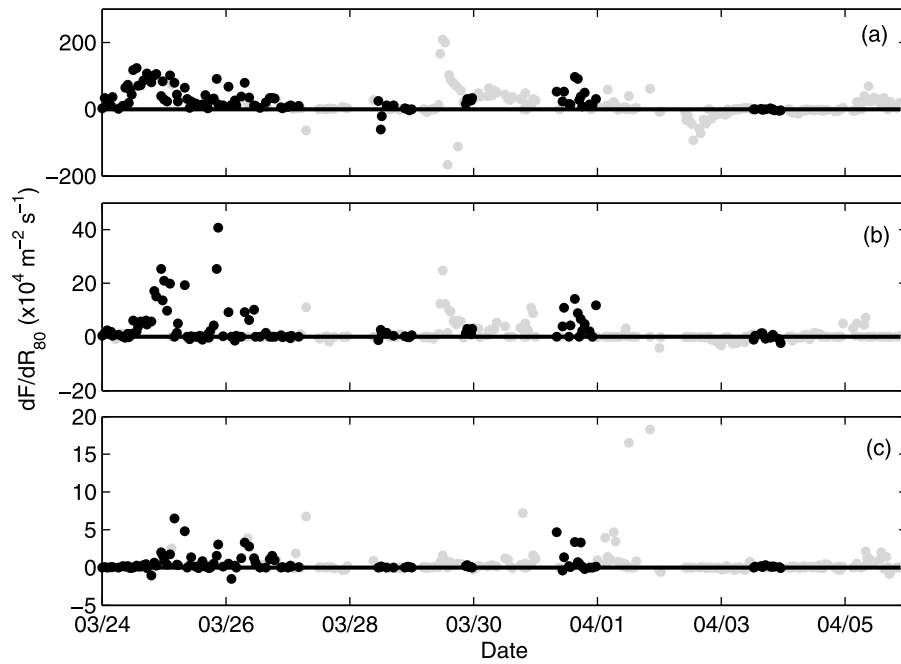


Figure 6. Time series for three channels: (a) mean $R_{80} = 0.9 \mu\text{m}$ (channel range $0.41\text{--}1.4 \mu\text{m}$), (b) $R_{80} = 1.9 \mu\text{m}$ ($1.8\text{--}2.0 \mu\text{m}$), and (c) $R_{80} = 2.6 \mu\text{m}$ ($2.4\text{--}2.8 \mu\text{m}$). Black dots meet quality control criteria; gray dots do not.

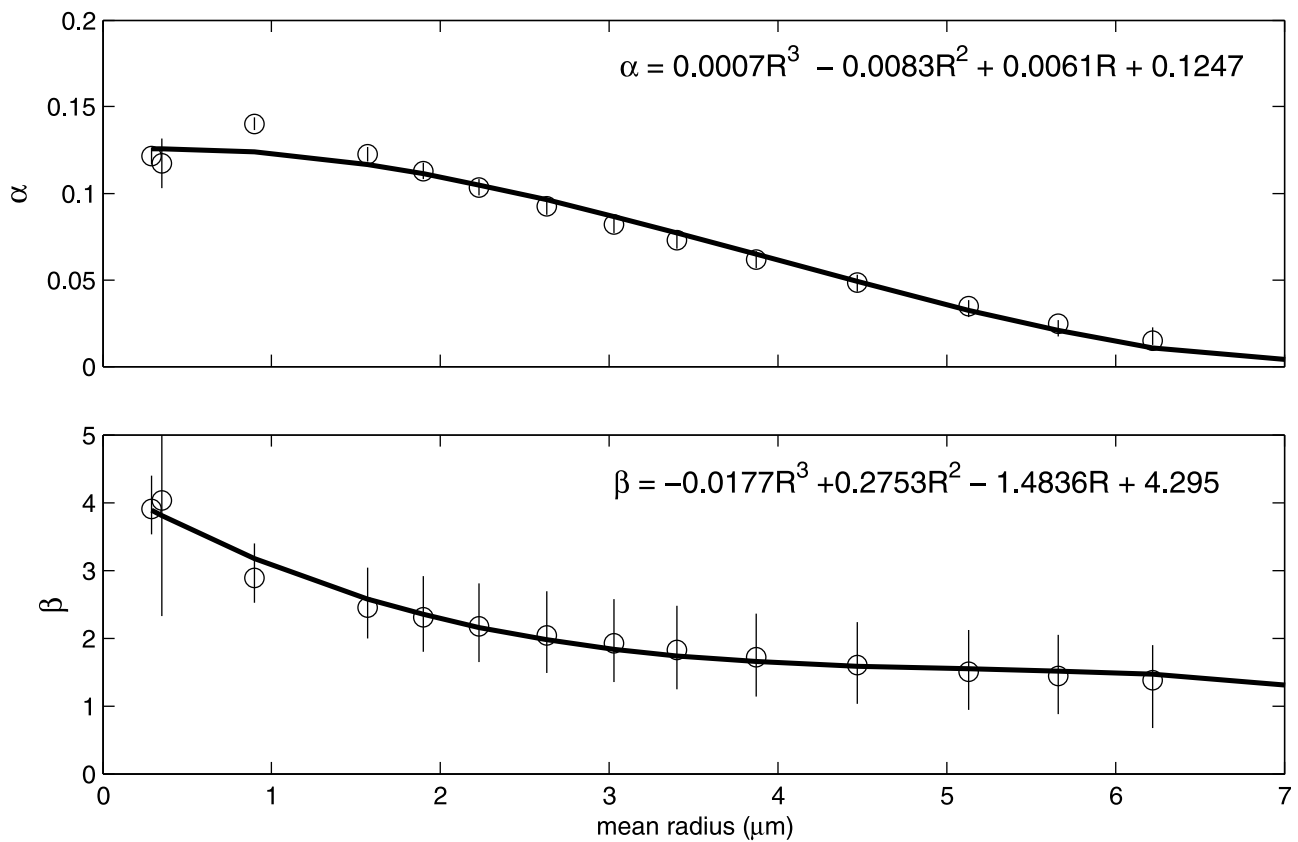


Figure 7. Fits to the coefficients α and β for the net flux in equation (2). Radius is at 80% humidity. The error bars show the 95% confidence on the coefficients α and β for each particles size range.

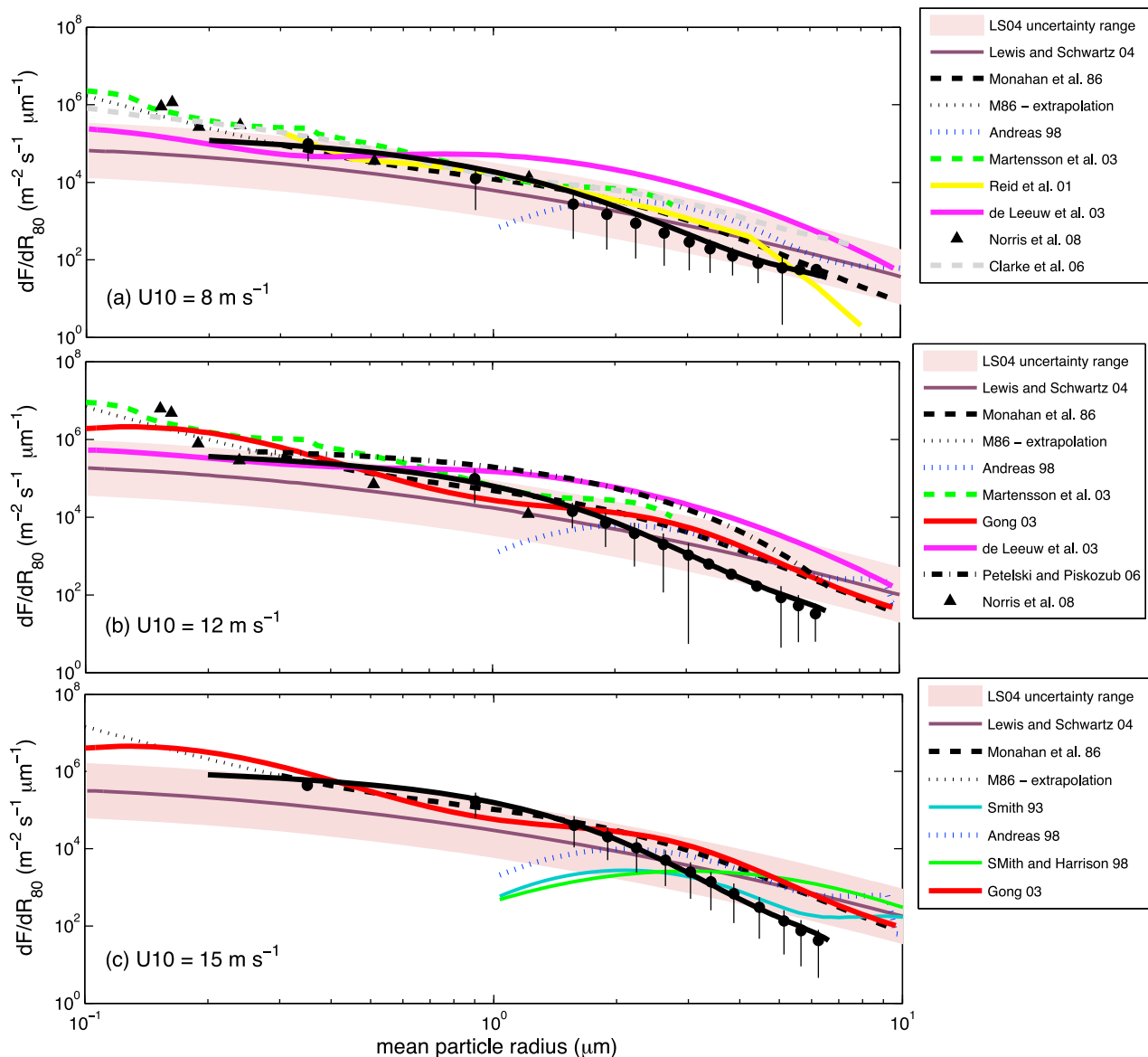


Figure 8. Comparison of the particle source fluxes normalized to a relative humidity of 80% with those from other recent studies at 10 m wind speeds of 8, 12, and 15 m s⁻¹. The standard deviations of the fluxes within each particle size bin are shown for each wind speed. The purple shaded area is the range of uncertainty (a factor of ~5) associated with the best estimate of the source flux determined by *Lewis and Schwartz* [2004] on the basis of a wide range of previous studies utilizing a variety of different techniques. Individual source functions are shown only for conditions within the particle size and wind speed ranges from which they were originally derived.

3.2. Eddy Covariance Fluxes

[22] Figure 6 shows a time series of individual estimates of the number flux for three different channels, with mean $R_{80} = 0.9$ (0.41–1.4), $R_{80} = 1.9$ (1.8–2.0) and $R_{80} = 2.6$ (2.4–2.8) μm , for both accepted (black) and rejected (gray) flux estimates (the rather large width of the first of these channels results from the use of a rough calibration when initially configuring the channel boundaries for the CLASP pulse height analyzer prior to the cruise). For all size channels the accepted flux estimates are dominated by positive (upward) fluxes. The ratio of positive to negative fluxes decreases with increasing particle size. For each CLASP channel the fit

to the flux (dF_{net}/dR) is an exponential function of the 10 m wind speed (U_{10})

$$\log\left(\frac{dF_{net}}{dR}\right) = \alpha U_{10} + \beta \quad (2)$$

[23] Polynomial fits to the coefficients α and β are then found as functions of particle size, R_{80} (μm), (Figure 7):

$$\begin{aligned} \alpha &= 0.0007R^3 - 0.0083R^2 + 0.0061R + 0.1247 \\ \beta &= -0.0177R^3 + 0.2753R^2 - 1.4836R + 4.295 \end{aligned} \quad (3)$$

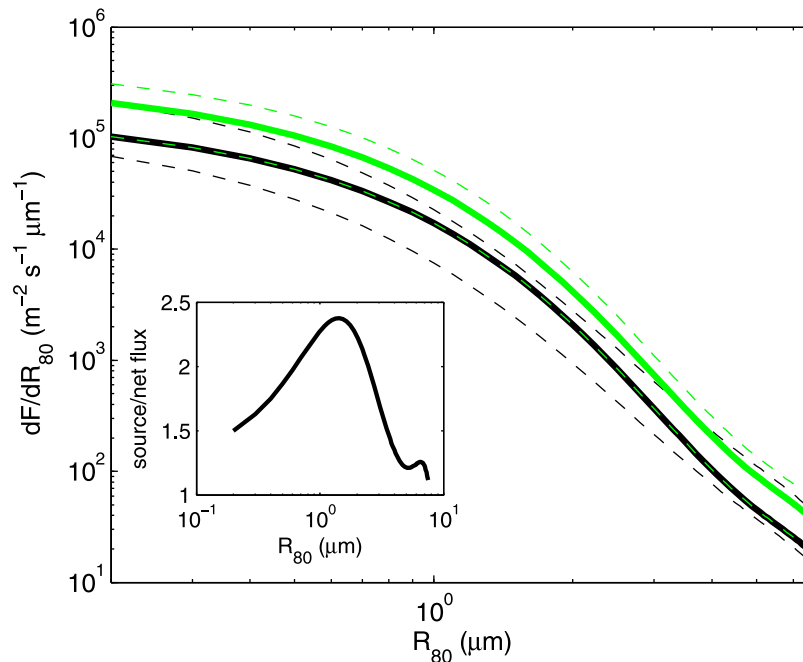


Figure 9. A comparison at 80% humidity of the source function from the eddy covariance method (solid green line) with the net eddy covariance function (solid black line) at 9 m s^{-1} . The standard errors for both curves are depicted by the dashed lines in their respective colors. The inset shows the ratio between the deposition-corrected eddy covariance flux and the net eddy covariance flux.

[24] The eddy covariance fluxes from which this function is derived are strictly estimates of the net flux – the sum of production and deposition fluxes – not the surface source. In order to make a best estimate of the source flux we correct each of our eddy covariance estimates for deposition using the deposition model of *Zhang et al.* [2001] for the deposition velocity (V_d), this deposition velocity model includes a roughness length as a function of wind speed for water surfaces.

$$\frac{dF_{\text{source}}}{dR} = \frac{dF_{\text{net}}}{dR} + \left(\frac{dN}{dR} \times V_d \right) \quad (4)$$

[25] The source function was calculated as for the net flux. The coefficients, as functions of particle size R_{80} (μm) of this best estimate of the source function are

$$\alpha = -0.000246R^4 + 0.0042R^3 - 0.0256R^2 + 0.0419R + 0.1116$$

$$\beta = -0.01R^3 + 0.2059R^2 - 1.37R + 4.391 \quad (5)$$

[26] This function is compared with a variety of source functions from other recent studies for mean 10 m s^{-1} in Figure 8. All the source functions are shown for particle sizes normalized to 80% relative humidity. The function obtained here lies within the range of the other functions for particles smaller than about $1 \mu\text{m}$, but decreases more rapidly with particle size at larger sizes, falling below most of the other functions for $R_{80} > 2 \mu\text{m}$.

[27] The deposition corrected flux is a factor of 1.2 to 2.5 larger than the net flux, increasing with size for particles with $R_{80} < \sim 1.5 \mu\text{m}$, then decreasing again for particles up to $R_{80} \sim 5 \mu\text{m}$ (Figure 9). This behavior results from the

combined influence of increasing deposition velocity but decreasing concentration with increasing particle size.

[28] The aerosol flux estimates for particles with R_{80} from 0.176 to $6.61 \mu\text{m}$, averaged in 1 m s^{-1} wind speed bins, are shown in Figure 10. There is a general increase in the estimated fluxes with wind speed up to about 13 m s^{-1} , with a flattening off or even decrease at higher wind speeds for particles larger than $0.9 \mu\text{m}$. This flattening off of the flux is also seen in the mean particle number concentrations as functions of wind speed (not shown). *Pant et al.* [2008] also reported a leveling off of particle concentration with wind speed for wind speeds between 16 and 22 m s^{-1} , as did *Exton et al.* [1985] between 14 and 19 m s^{-1} . *Pant et al.* [2008] suggested that the feature might be an inlet sampling efficiency issue at high wind speeds. Another possibility is that it results from a sampling bias due to the small number of observations at these higher wind speeds within each study. During an extended series of measurements in the Outer Hebrides, almost 30 years ago [*Smith et al.*, 1989], one of us (MHS) was struck by a leveling off of the particle concentrations at the highest wind speeds recorded; however, when further measurements extended to higher wind speeds, the earlier leveling off was not observed but a similar feature occurred at the new high wind speed limit. Although the issue was never pursued, a possible explanation was considered. In any given sample interval the mean wind speed and particle concentration are obtained; the equilibrium particle concentration will typically lag changes in the wind speed. For the majority of the wind speed range a more or less equal number of samples will be obtained from intervals with increasing/decreasing wind, and the effect of the lag on particle concentration is averaged out. At the

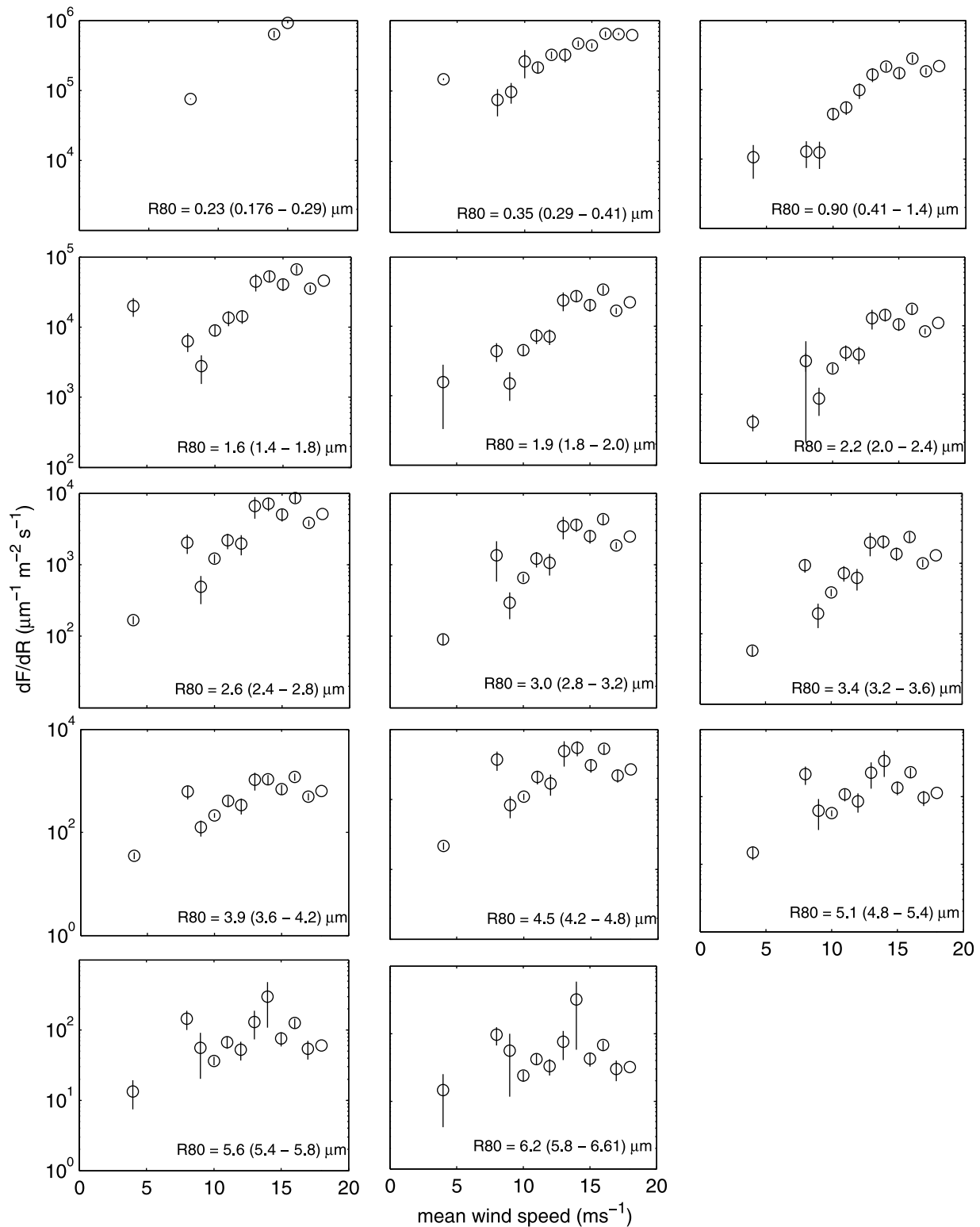


Figure 10. Variation of eddy covariance fluxes with wind speed for each particle size range. The error bars show the standard error of the data in each wind speed bin.

highest wind speeds, there are no sample intervals with decreasing wind speeds, and the bias introduced by the lag becomes significant. To account for this effect both the nonlinear relationships between source function and wind

speed and the time constants for different particle sizes to approach equilibrium would need to be taken into account. [29] The explanation above applies to measurements of mean concentrations and source functions derived from

them via the equilibrium method. It would not apply to direct flux estimates if the surface source responds to the wind forcing on a time scale shorter than the averaging time. If the response of spray production from whitecaps lags changes in the wind by much more than the flux averaging time, then a similar bias would apply. This would be the case if wave state is a significant controlling factor on white capping; this is discussed further in section 4.

4. Discussion

[30] The measured eddy covariance flux is a reasonable approximation to the source flux only if deposition is much less than production. The correction of the net eddy covariance fluxes for deposition relies upon the choice of deposition model. A wide range of deposition models have been defined, with the majority based on those by *Slinn et al.* [1978], *Slinn* [1983], and *Slinn and Slinn* [1980]; these span an order of magnitude or more for particles with $R < 1 \mu\text{m}$ at 80% relative humidity, and a factor of several for larger particles [*Lewis and Schwartz*, 2004]. The model of *Zhang et al.* [2001] used here includes a roughness length as a function of wind speed and for water surfaces; however, both it and other available functions are derived largely from theoretical considerations and have not been verified by direct measurement.

[31] The source function derived using the eddy covariance technique, defined by (4) and (5) and shown in Figure 8 starts to fall below that from previous studies for particles larger than about $2 \mu\text{m}$ radius; the difference is greater than one standard deviation in our flux estimates for most of these larger particles. It is not immediately clear if this decrease represents the true behavior of the particle flux, or if it is a result of a measurement bias.

[32] The source function made here is valid for the measurement height whereas some of the functions in Figure 8 are interfacial estimates and some are effective fluxes [*Reid et al.*, 2001; *Lewis and Schwartz*, 2004; *Norris et al.*, 2008]. The interfacial flux is defined as the flux of those particles leaving the sea surface, whereas the effective function is defined as the flux of those particles that attain a certain height, typically 10 m [*de Leeuw et al.*, 2011]. For particles with $R_{80} > 1 \mu\text{m}$ the effective flux becomes increasingly less than the interfacial flux with increasing particle size. This difference between the interfacial fluxes and our effective flux may account for some or all of the difference between our estimates and other functions for $R_{80} > 2 \mu\text{m}$.

[33] A potential source of bias is the sampling efficiency of the inlet as a function of wind speed and flow orientation [*Davies and Subari*, 1982]; however, agreement, within a factor of 2, with an independent measurement of the mean size spectra from a PCASP gives confidence in the CLASP size spectra. A test was performed during a land-based campaign in the UK with two CLASP units with inlets orientated at 180 degrees to each other. The spectra from the two units showed no significant differences, suggesting any bias in sampling efficiency due to orientation with respect to the mean wind is negligible. Both wind speed and orientation-dependent sampling biases might be expected to show a periodicity due to ship motion, which should be evident at the wave scale (0.08–0.2 Hz [*Brooks*, 2008]) in an

examination of frequency-resolved flux contributions such as the ogive curves in Figure 3. There is some evidence of such a wave scale signal in some the ogives in Figure 3; however, it is small and we estimate would result in a reduction in the mean flux of no more than 5%. Another possibility that we cannot exclude is that the particle losses to the curved wall of the CLASP inlets have been inadequately corrected.

[34] The SEASAW results are the only ones shown in Figure 8 derived from measurements over the open ocean rather than a coastal environment or within a laboratory. In coastal waters, swell may undergo transformations by refraction, shoaling and breaking [*Mulligan et al.*, 2008], modifying wind-wave relationships compared to the open ocean; the fetch may be limited, and water properties such as temperature, salinity, and surfactant concentration, all of which affect whitecap and bubble properties and hence sea spray production, may differ from those in the open ocean. Sea spray production is directly related to whitecap coverage and bubble properties [*Monahan and Muircheartaigh*, 1980; *Monahan et al.*, 1983]. Parameterization of the sea spray aerosol flux in terms of U_{10} implicitly assumes that the sea state is in equilibrium with the wind; in practice this will rarely be the case. *Stramska and Petelski* [2003] found that for a given wind speed whitecap coverage was greater for well-developed seas than for undeveloped seas, assuming that the sea state was determined primarily by the duration of the wind forcing; this result is supported by the more recent study of *Goddijn-Murphy et al.* [2011].

[35] A useful measure of the state of development of the sea surface is the mean wave slope (or significant steepness),

$$\text{mean slope} = \frac{2\pi H_s}{gT_z^2}, \quad (6)$$

where T_z is the mean wave period and H_s is the significant wave height: slopes greater than 0.03 indicate an undeveloped sea state, those less than 0.03 indicate a well-developed sea [*Bourassa et al.*, 2001]. The mean wave slope corresponding to each aerosol flux estimate was calculated using data from a ship borne wave recorder [*Tucker and Pitt*, 2001; *Holliday et al.*, 2006]. Of the 111 data points used in this analysis 82 are from undeveloped seas while only 29 points are in conditions where the sea state can be described as being well developed or in equilibrium with the wind forcing. For wind speeds below about 7 m s^{-1} the observed sea states are all well developed, between 7 and 14 m s^{-1} a wide range of sea states was observed, and above 14 m s^{-1} only undeveloped sea states were encountered (Figure 11). These are similar wind speed ranges to those quoted by *Goddijn-Murphy et al.* [2011], who found that undeveloped sea states at higher wind speeds resulted in lower whitecap coverage than for well-developed seas at the same wind speed. Figure 11 shows example source flux estimates for two different size ranges plotted against wind speed and partitioned by wave state with best fit lines defined as in equation (2). Undeveloped wave states show a higher flux than fully developed wave states for $R_{80} > 0.4 \mu\text{m}$, by a factor of up to approximately 2.5; for smaller particles there is no difference in the flux with wave state. This result is surprising since the whitecap studies cited above found whitecap fractions to be higher for developed than undeveloped sea states. The scatter in the flux estimates, however, is large and

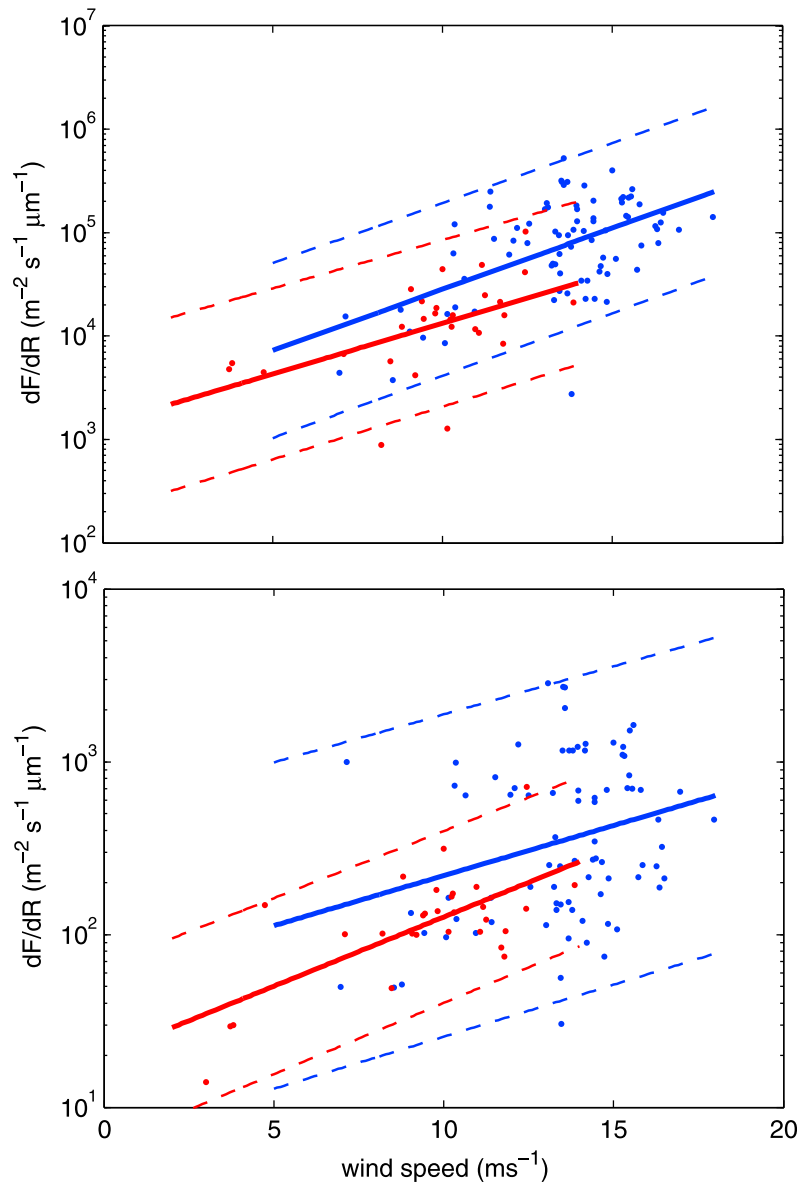


Figure 11. The effect of mean wave state on the particle flux variation with local 10 m wind speed for two contrasting particle sizes: (top) $R_{80} = 0.9 \mu\text{m}$ (0.41–1.4 μm) and (bottom) $R_{80} = 3.9 \mu\text{m}$ (3.6–4.2 μm). A mean wave slope of greater than 0.03 (blue) represents undeveloped seas; a value less than 0.03 (red) represents fully developed seas. The solid lines are the best fits (equation (2)), while the dashed lines represent the 95% confidence bounds on the fit.

the lines of best fit lie within each other's 95% confidence limits and cannot be judged significantly different. As for the fits to the whole data set (Figure 7) most of the uncertainty lies in the mean offset (β) and the gradients are found to be significantly different. Figure 12 shows the gradient of these fits (α in equation (2)) for each CLASP channel. The best fit gradients for both developed and undeveloped sea states are size dependent, decreasing with increasing particle size for $R_{80} > 1 \mu\text{m}$. For particles with $R_{80} > 2.5 \mu\text{m}$ α has a higher magnitude for developed sea states than for undeveloped sea states suggesting that developed sea states have a stronger response to the wind speed. The weaker response to wind speed at larger particle sizes under undeveloped seas is a potential contributing factor for the SEASAW source function dropping

increasingly below other functions for larger particles with increasing wind speeds. Few previous studies of sea spray production have included detailed information on wave state; it is thus very difficult to assess how much this factor may contribute to the differences between studies; however, there is increasing evidence to suggest that it may be an important controlling factor.

[36] While eddy covariance provides the most direct measure of any flux, its application to aerosols is more complicated than for heat, water vapor, or trace gases. Some of the practical problems relating to the application of eddy covariance to aerosol fluxes are discussed above; others, less tractable in nature have been neglected. These include the gravitational sedimentation velocity and inertia of particles,

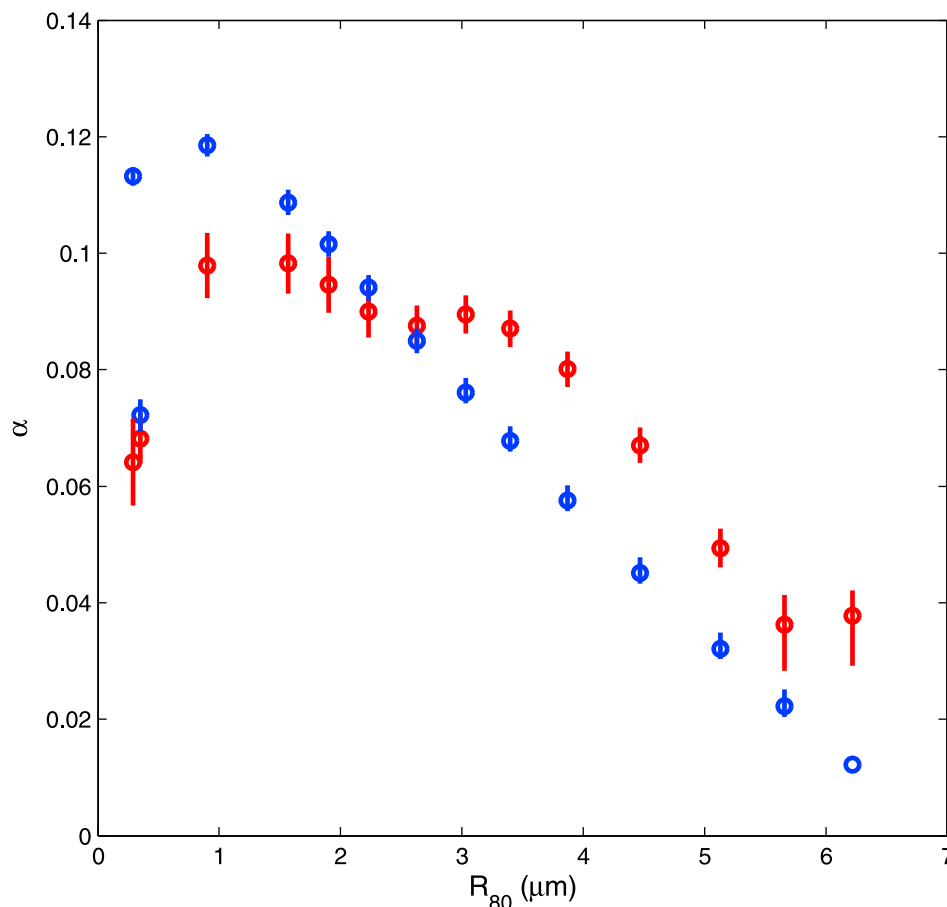


Figure 12. A comparison between the gradient, α , of the linear fit of the log of the aerosol flux with mean 10 m wind speed for well-developed (red circles) and undeveloped (blue circles) sea states. The error bars show the 95% confidence limits for α .

both of which may result in departures of particle motion from the measured turbulent air motion [Brooks *et al.*, 2011]. Neither of these factors has been quantified to date, but would increase in importance with increasing particle size. Neither is likely to be significant for the submicron particles that make up the majority of the fluxes measured here, but are a potential source of bias for the larger particles. We note that both are likely to reduce the actual flux and hence their neglect should mean our flux estimates are slightly overestimated for large particles and thus cannot explain the shortfall compared to other source functions for large particles. A further issue is that the use of eddy covariance measurements to derive a flux parameterization relies upon the tenets of Monin-Obukhov similarity theory: namely, that the eddy covariance flux is constant with height near the sea surface when conditions are stationary and horizontally homogeneous, and that the vertical gradient in concentration can be related to the surface flux. Neither of these assumptions has yet been validated for aerosol fluxes.

5. Summary and Conclusions

[37] We have presented direct eddy covariance estimates of size-segregated sea spray aerosol fluxes for the size range $0.176 < R_{80} < 6.61 \mu\text{m}$ over the open ocean. The observations cover a range of mean wind speeds from 4 to 18 m s^{-1} .

Both the net flux and the particle source function have been parameterized as exponential functions of the 10 m wind speed. The source function lies within the range of recent estimates of the source function for particle sizes between approximately 0.1 and $1 \mu\text{m}$ but falls increasingly below them with increasing wind speed for particles larger than $2 \mu\text{m}$. This increasing discrepancy from previous source functions is hard to explain; it might be real and result from conditions encountered in the open ocean, but we cannot exclude the possibility that it is an artifact of the measurements. Decreasing particle concentration with size results in increasingly poor sampling statistics; this limits the effectiveness of the eddy covariance measurements to particles smaller than about $5 \mu\text{m}$ (ambient radius).

[38] We find some evidence for the influence of sea state on the particle flux, notably that the source flux response to increasing wind appears stronger for full developed than for undeveloped sea states for particles with $R_{80} > 2.5 \mu\text{m}$. The volume of data is limited however, and a larger data set is required to establish functional relationships.

[39] **Acknowledgments.** SEASAW was funded by the UK Natural Environment Research Council, grants NE/C001842/1 and NE/G000107/1, as part of UK SOLAS. We would like to thank Captain Roger Chamberlain and the crew of the RRS *Discovery*, along with the staff of National Marine Facilities Sea Systems, for their assistance preparing for and during the cruises.

References

- Andreas, E. L. (1998), A new sea spray generation function for wind speeds up to 32 m s^{-1} , *J. Phys. Oceanogr.*, **28**, 2175–2184, doi:10.1175/1520-0485(1998)028<2175:ANSSGF>2.0.CO;2.
- Andreas, E. L. (2002), A review of the sea spray generation function for the open ocean, in *Atmosphere-Ocean Interactions*, vol. 1, edited by W. Perrie, pp. 1–46, WIT Press, Southampton, U. K.
- Andreas, E. L. (2007), Comment on “Vertical coarse aerosol fluxes in the atmospheric surface layer over the North Polar Waters of the Atlantic” by Tomasz Petelski and Jacek Piskozub, *J. Geophys. Res.*, **112**, C11010, doi:10.1029/2007JC004184.
- Anguelova, M. D., and F. Webster (2006), Whitecap coverage from satellite measurements: A first step toward modeling the variability of oceanic whitecaps, *J. Geophys. Res.*, **111**, C03017, doi:10.1029/2005JC003158.
- Bourassa, M. A., D. G. Vincent, and W. L. Wood (2001), A sea state parameterization with nonarbitrary wave age applicable to low and moderate wind speeds, *J. Phys. Oceanogr.*, **31**, 2840–2851, doi:10.1175/1520-0485(2001)031<2840:ASSPWN>2.0.CO;2.
- Brooks, I. M. (2008), Spatially distributed measurements of platform motion for the correction of ship-based turbulent fluxes, *J. Atmos. Oceanic Technol.*, **25**, 2007–2017, doi:10.1175/2008JTECHA1086.1.
- Brooks, I. M., and D. P. Rogers (2000), Aircraft observations of the mean and turbulent structure of a shallow boundary layer over the Persian Gulf, *Boundary Layer Meteorol.*, **95**, 189–210, doi:10.1023/A:1002623712237.
- Brooks, I. M., et al. (2009), Physical exchanges at the air-sea interface: Field measurements from UK-SOLAS, *Bull. Am. Meteorol. Soc.*, **90**, 629–644, doi:10.1175/2008BAMS2578.1.
- Brooks, I. M., E. L. Andreas, G. McFiggins, M. D. Anguelova, and C. D. O’Dowd (2011), Primary marine aerosol fluxes: Progress and priorities, *Bull. Am. Meteorol. Soc.*, **92**(4), 489–491, doi:10.1175/2010BAMS3112.1.
- Buzorius, G., Ü. Rannik, J. M. Makela, P. Keronen, T. Vesala, and M. Kulmala (2000), Vertical aerosol fluxes measured by the eddy covariance method and deposition of nucleation mode particles above a Scots pine forest in southern Finland, *J. Geophys. Res.*, **105**, 19,905–19,916, doi:10.1029/2000JD900108.
- Clarke, A. D., S. R. Owens, and J. Zhou (2006), An ultrafine sea-salt flux from breaking waves: Implications for cloud condensation nuclei in the remote marine atmosphere, *J. Geophys. Res.*, **111**, D06202, doi:10.1029/2005JD006565.
- Davies, C. N., and M. Subari (1982), Aspiration above wind velocity of aerosols with thin-walled nozzles facing and at right angles to the wind direction, *J. Aerosol Sci.*, **13**(1), 59–71, doi:10.1016/0021-8502(82)90008-8.
- de Leeuw, G., M. Moerman, L. Cohen, B. Brooks, M. Smith, and E. Vignati (2003), Aerosols, bubbles and sea spray production studies during the RED experiments, paper presented at Third Conference on Artificial Intelligence Applications to Environmental Sciences, Am. Meteorol. Soc., Long Beach, Calif., 9–13 Feb.
- de Leeuw, G., M. M. Moerman, C. J. Zappa, W. R. McGillis, S. J. Norris, and M. H. Smith (2007), Eddy correlation measurements of sea spray aerosol fluxes, in *Transport at the Air Sea Interface*, edited by C. S. Garbe, R. A. Handler, and B. Jähne, pp. 297–311, Springer, Berlin, doi:10.1007/978-3-540-36906-6_21.
- de Leeuw, G., E. L. Andreas, M. D. Anguelova, C. W. Fairall, E. R. Lewis, C. O’Dowd, M. Schulz, and S. E. Schwartz (2011), Production flux of sea-spray aerosol, *Rev. Geophys.*, **49**, RG2001, doi:10.1029/2010RG000349.
- Doss-Hammel, S. M., C. R. Zeisse, A. E. Barrios, G. de Leeuw, M. Moerman, A. N. de Jong, P. A. Frederickson, and K. L. Davidson (2002), Low-altitude infrared propagation in a coastal zone: Refraction and scattering, *Appl. Opt.*, **41**, 3706–3724, doi:10.1364/AO.41.003706.
- Edson, J. B., A. A. Hinton, K. E. Prada, J. E. Hare, and C. W. Fairall (1998), Direct covariance flux estimates from mobile platforms at sea, *J. Atmos. Oceanic Technol.*, **15**, 547–562, doi:10.1175/1520-0426(1998)015<0547:DCFEM>2.0.CO;2.
- Exton, H. J., J. Latham, P. M. Park, S. J. Perry, M. H. Smith, and R. R. Allan (1985), The production and dispersal of marine aerosol, *Q. J. R. Meteorol. Soc.*, **111**, 817–837, doi:10.1256/smsqj.46908.
- Fairall, C. W. (1984), Interpretation of eddy-correlation measurements of particulate deposition and aerosol flux, *Atmos. Environ.*, **18**, 1329–1337, doi:10.1016/0004-6981(84)90041-6.
- Fairall, C. W., and S. E. Larsen (1984), Dry deposition, surface production and dynamics of aerosols in the marine boundary layer, *Atmos. Environ.*, **18**, 69–77, doi:10.1016/0004-6981(84)90229-4.
- Fairall, C. W., K. L. Davidson, and G. E. Schaucher (1983), An analysis of the surface production of sea-salt aerosol, *Tellus, Ser. B*, **35**, 31–39, doi:10.1111/j.1600-0889.1983.tb00005.x.
- Fairall, C. W., A. B. White, J. B. Edson, and J. E. Hare (1997), Integrated shipboard measurements of the marine boundary layer, *J. Atmos. Oceanic Technol.*, **14**, 338–359, doi:10.1175/1520-0426(1997)014<0338:ISMOTM>2.0.CO;2.
- Friehe, C. A., W. J. Shaw, D. P. Rogers, K. L. Davidson, W. G. Large, S. A. Stage, G. H. Crescenti, S. J. S. Khalsa, G. K. Greenhut, and F. Li (1991), Air-sea fluxes and surface layer temperatures around a sea-surface temperature front, *J. Geophys. Res.*, **96**, 8593–8609, doi:10.1029/90JC02062.
- Geever, M. C., D. O’Dowd, S. van Ekeren, R. Flanagan, E. D. Nilsson, G. de Leeuw, and Ü. Rannik (2005), Submicron sea spray fluxes, *Geophys. Res. Lett.*, **32**, L15810, doi:10.1029/2005GL023081.
- Goddijn-Murphy, L., D. K. Woolf, and A. H. Callaghan (2011), Parameterizations and algorithms for oceanic whitecap coverage, *J. Phys. Oceanogr.*, **41**, 742–756, doi:10.1175/2010JPO4533.1.
- Gong, S. L. (2003), A parameterization of sea-salt aerosol source function for sub- and super-micron particles, *Global Biogeochem. Cycles*, **17**(4), 1097, doi:10.1029/2003GB002079.
- Haywood, J. M., V. Ramaswamy, and B. J. Soden (1999), Tropospheric aerosol climate forcing in clear-sky satellite observations over the oceans, *Science*, **283**, 1299–1303, doi:10.1126/science.283.5406.1299.
- Held, A., I. M. Brooks, C. Leck, and M. Tjernström (2011), On the potential contribution of open lead particle emissions to the central Arctic aerosol concentration, *Atmos. Chem. Phys.*, **11**, 3093–3105, doi:10.5194/acp-11-3093-2011.
- Hill, M. K., B. J. Brooks, S. J. Norris, M. H. Smith, I. M. Brooks, G. de Leeuw, and J. J. N. Lingard (2008), A Compact Lightweight Aerosol Spectrometer Probe (CLASP), *J. Atmos. Oceanic Technol.*, **25**, 1996–2006, doi:10.1175/2008JTECHA1051.1.
- Holliday, N. P., M. J. Yelland, R. W. Pascal, V. R. Swail, P. K. Taylor, C. R. Griffiths, and E. C. Kent (2006), Were extreme waves in the Rockall Trough the largest ever recorded?, *Geophys. Res. Lett.*, **33**, L05613, doi:10.1029/2005GL025238.
- Hoppel, W. A., G. M. Frick, and J. W. Fitzgerald (2002), The surface source function for sea-salt aerosol and aerosol dry deposition to the ocean surface, *J. Geophys. Res.*, **107**(D19), 4382, doi:10.1029/2001JD002014.
- Horst, T. W. (1997), A simple formula for attenuation of eddy fluxes measured with first-order-response scalar sensors, *Boundary Layer Meteorol.*, **82**, 219–233, doi:10.1023/A:1000229130034.
- Kowalski, A. S. (2001), Deliquescence induces eddy covariance and estimable dry deposition errors, *Atmos. Environ.*, **35**, 4843–4851, doi:10.1016/S1352-2310(01)00270-9.
- Lewis, E. R., and S. E. Schwartz (2004), *Sea Salt Aerosol Production: Mechanisms, Methods, Measurements, and Models—A Critical Review*, *Geophys. Monogr. Ser.*, vol. 152, 413 pp., AGU, Washington, D. C.
- Lewis, E. R., and S. E. Schwartz (2006), Comment on “Size distribution of sea-salt emissions as a function of relative humidity,” *Atmos. Environ.*, **40**, 588–590, doi:10.1016/j.atmosenv.2005.08.043.
- Mårtensson, E. M., E. D. Nilsson, G. de Leeuw, L. H. Cohen, and H. C. Hansson (2003), Laboratory simulations and parameterization of the primary marine aerosol production, *J. Geophys. Res.*, **108**(D9), 4297, doi:10.1029/2002JD002263.
- Monahan, E. C., and I. O. Muircheartaigh (1980), Optimal power-law description of oceanic whitecap coverage dependence on wind speed, *J. Phys. Oceanogr.*, **10**, 2094–2099, doi:10.1175/1520-0485(1980)010<2094:OPLDOO>2.0.CO;2.
- Monahan, E. C., D. E. Spiel, and K. L. Davidson (1982), Whitecap aerosol productivity deduced from simulation tank measurements, *J. Geophys. Res.*, **87**, 8898–8904, doi:10.1029/JC087C11p08898.
- Monahan, E. C., C. W. Fairall, K. L. Davidson, and P. J. Boyle (1983), Observed inter relationships amongst 10m-elevation winds, oceanic whitecaps, and marine aerosols, *Q. J. R. Meteorol. Soc.*, **109**, 379–392, doi:10.1002/qj.49710946010.
- Monahan, E. C., D. E. Spiel, and K. L. Davidson (1986), A model of marine aerosol generation via whitecaps and wave disruption, in *Oceanic Whitecaps*, edited by E. C. Monahan and G. Mac Niocaill, pp. 167–174, D. Reidel, Dordrecht, Netherlands, doi:10.1007/978-94-009-4668-2_16.
- Mulligan, R. P., A. J. Bowen, A. E. Hay, A. J. van der Westhuysen, and J. A. Battjes (2008), Whitecapping and wave field evolution in a coastal bay, *J. Geophys. Res.*, **113**, C03008, doi:10.1029/2007JC004382.
- Nilsson, E. D., Ü. Rannik, E. Swietlicki, C. Leck, P. P. Aalto, J. Zhou, and M. Norman (2001), Turbulent aerosol fluxes over the Arctic Ocean: 2. Wind-driven sources from the sea, *J. Geophys. Res.*, **106**, 32,139–32,154, doi:10.1029/2000JD900747.
- Norris, S. J., I. M. Brooks, G. de Leeuw, M. H. Smith, M. Moerman, and J. J. N. Lingard (2008), Eddy covariance measurements of sea spray particles over the Atlantic Ocean, *Atmos. Chem. Phys.*, **8**, 555–563, doi:10.5194/acp-8-555-2008.
- O’Dowd, C. D., and G. de Leeuw (2007), Marine aerosol production: A review of the current knowledge, *Philos. Trans. R. Soc. A*, **365**, 1753–1774, doi:10.1098/rsta.2007.2043.

- O'Dowd, C. D., J. A. Lowe, and M. H. Smith (1999), Coupling of sea-salt and sulphate interactions and its impact on cloud droplet concentration predictions, *Geophys. Res. Lett.*, *26*, 1311–1314, doi:10.1029/1999GL900231.
- O'Dowd, C. D., J. A. Lowe, N. Clegg, M. H. Smith, and S. L. Clegg (2000), Modeling heterogeneous sulphate production in maritime stratiform clouds, *J. Geophys. Res.*, *105*(D6), 7143–7160, doi:10.1029/1999JD900915.
- Pant, V., C. G. Deshpande, and A. K. Kamra (2008), On the aerosol number concentration–wind speed relationship during a severe cyclonic storm over south Indian Ocean, *J. Geophys. Res.*, *113*, D02206, doi:10.1029/2006JD008035.
- Petelski, T., and J. Piskozub (2006), Vertical coarse aerosol fluxes in the atmospheric surface layer over the north polar waters of the Atlantic, *J. Geophys. Res.*, *111*, C06039, doi:10.1029/2005JC003295.
- Pui, D. Y. H., F. Romay-Novas, and B. Y. H. Lui (1987), Experimental study of particle deposition in bends of circular cross section, *Aerosol Sci. Technol.*, *7*, 301–315, doi:10.1080/02786828708959166.
- Reid, J. S., H. H. Jonsson, M. H. Smith, and A. Smirnov (2001), Evolution of the vertical profile and flux of large sea-salt particles in a coastal zone, *J. Geophys. Res.*, *106*, 12,039–12,053, doi:10.1029/2000JD900848.
- Saxena, P., and L. Hildemann (1996), Water-soluble organics in atmospheric particles: A critical review of the literature and application of thermodynamics to identify candidate compounds, *J. Atmos. Chem.*, *24*, 57–109, doi:10.1007/BF00053823.
- Saxena, P., L. Hildemann, P. H. McMurry, and J. H. Seinfeld (1995), Organics alter hygroscopic behavior of atmospheric particles, *J. Geophys. Res.*, *100*, 18,755–18,770, doi:10.1029/95JD01835.
- Slinn, S. A., and W. G. N. Slinn (1980), Predictions for particle deposition on natural water, *Atmos. Environ.*, *14*, 1013–1016, doi:10.1016/0004-6981(80)90032-3.
- Slinn, W. G. N. (1983), Air to sea transfer of particles, in *Air Sea Exchange of Gases and Particles*, edited by P. S. Liss and W. G. N. Slinn, pp. 299–405, D. Reidel, Dordrecht, Netherlands.
- Slinn, W. G. N., L. Hasse, B. B. Hicks, A. W. Hogan, D. Lal, P. S. Liss, K. O. Munnich, G. A. Sehmel, and O. Vittori (1978), Some aspects of the transfer of atmospheric trace constituents past the air-sea interface, *Atmos. Environ.*, *12*, 2055–2087, doi:10.1016/0004-6981(78)90163-4.
- Smith, M. H., and N. M. Harrison (1998), The sea spray generation function, *J. Aerosol Sci.*, *29*, Suppl. 1, S189–S190.
- Smith, M. H., P. M. Park, and I. E. Consterdine (1989), Atmospheric loadings of marine aerosol during a Hebridean cyclone, *Q. J. R. Meteorol. Soc.*, *115*, 383–395, doi:10.1002/qj.49711548610.
- Smith, M. H., P. M. Park, and I. E. Consterdine (1993), Marine aerosol concentrations and estimated fluxes over the ocean, *Q. J. R. Meteorol. Soc.*, *119*, 809–824, doi:10.1002/qj.49711951211.
- Sørensen, L. L., S. Pryor, G. de Leeuw, and M. Schulze (2005), Flux divergence for nitric acid in the marine atmospheric surface layer, *J. Geophys. Res.*, *110*, D15306, doi:10.1029/2004JD005403.
- Stramska, M., and T. Petelski (2003), Observations of oceanic whitecaps in the north polar waters of the Atlantic, *J. Geophys. Res.*, *108*(C3), 3086, doi:10.1029/2002JC001321.
- Swietlicki, E., et al. (1999), A closure study of sub-micrometer aerosol particle hygroscopic behavior, *Atmos. Res.*, *50*, 205–240, doi:10.1016/S0169-8095(98)00105-7.
- Tang, I. N., A. C. Tridico, and K. H. Fung (1997), Thermodynamic and optical properties of sea salt aerosols, *J. Geophys. Res.*, *102*(D19), 23,269–23,275, doi:10.1029/97JD01806.
- Tucker, M. J., and E. G. Pitt (2001), *Waves in Ocean Engineering, Ocean Eng. Book Ser.*, vol. 5, 521 pp., Elsevier, New York.
- Webb, E. K., G. I. Pearman, and R. Leuning (1980), Correction of flux measurements for density effects due to heat and water vapour transfer, *Q. J. R. Meteorol. Soc.*, *106*, 85–100, doi:10.1002/qj.49710644707.
- Yelland, M. J., B. I. Moat, P. K. Taylor, R. W. Pascal, J. Hutchings, and V. C. Cornell (1998), Wind stress measurements from the open ocean corrected for air flow distortion by the ship, *J. Phys. Oceanogr.*, *28*, 1511–1526, doi:10.1175/1520-0485(1998)028<1511:WSMFTO>2.0.CO;2.
- Yelland, M. J., B. I. Moat, R. W. Pascal, and D. I. Berry (2002), CFD model estimates of the airflow distortion over research ships and the impact on momentum flux measurements, *J. Atmos. Oceanic Technol.*, *19*, 1477–1499, doi:10.1175/1520-0426(2002)019<1477:CMEOTA>2.0.CO;2.
- Yelland, M. J., R. W. Pascal, P. K. Taylor, and B. I. Moat (2009), AutoFlux: An autonomous system for the direct measurement of the air-sea fluxes of CO₂, heat and momentum, *J. Oper. Oceanogr.*, *2*, 15–23.
- Zhang, L., S. Gong, J. Padro, and L. Barrie (2001), A size-segregated particle dry deposition scheme for an atmospheric aerosol module, *Atmos. Environ.*, *35*, 549–560, doi:10.1016/S1352-2310(00)00326-5.

B. J. Brooks, I. M. Brooks, M. K. Hill, S. J. Norris, M. H. Smith, and D. A. J. Sproson, School of Earth and Environment, University of Leeds, Leeds LS2 9JT, UK. (s.norris@see.leeds.ac.uk)